IOPscience iopscience.iop.org

Home Search Collections Journals About Contact us My IOPscience

Magnetism and Hund's rule in an optical lattice with cold fermions

This content has been downloaded from IOPscience. Please scroll down to see the full text.

2007 New J. Phys. 9 33

(http://iopscience.iop.org/1367-2630/9/2/033)

View the table of contents for this issue, or go to the journal homepage for more

Download details:

IP Address: 152.78.130.228
This content was downloaded on 29/07/2014 at 13:47

Please note that terms and conditions apply.

New Journal of Physics
The open–access journal for physics

Magnetism and Hund's rule in an optical lattice with cold fermions

K Kärkkäinen[1], M Borgh[1], M Manninen[2] and S M Reimann[1]

[1] Mathematical Physics, LTH, Lund University, SE-22100, Lund, Sweden
[2] NanoScience Centre, Department of Physics, University of Jyväskylä, FIN-40351, Finland
E-mail: reimann@matfys.lth.se

New Journal of Physics **9** (2007) 33
Received 6 November 2006
Published 21 February 2007
Online at http://www.njp.org/
doi:10.1088/1367-2630/9/2/033

Abstract. We demonstrate that a two-dimensional (2D) optical lattice loaded with repulsive, contact-interacting fermions shows a rich and systematic magnetic phase diagram. Trapping a few ($N \leqslant 12$) fermions in each of the single-site minima of the optical lattice, we find that the *shell structure* in these quantum wells determines the magnetism. In a shallow lattice, the tunnelling between the single wells is strong, and the lattice is non-magnetic (NM). For deeper lattices, however, the shell filling of the single wells with fermionic atoms determines the magnetism. As a consequence of Hund's first rule, the interaction energy is lowered by maximizing the number of atoms of the same species. This leads to a systematic sequence of NM, ferromagnetic (F) and antiferromagnetic (AF) phases.

Artificially confined, small quantal systems exhibit a high potential for employing quantum physics in technology. Ultra-cold atom gases have opened an exciting laboratory to explore many-particle systems that are not accessible in conventional atomic or solid state physics. It appears promising that the optical trapping of cold bosonic or fermionic atoms makes possible the future construction of devices with unprecedented precision, allowing experimenters to make the samples much more 'clean'—and thus more coherent. Trapped atomic quantum gases may thus provide an interesting alternative to the quantum dot nanostructures [1] made today. Optical lattices created by standing laser waves loaded with ultra-cold atoms are such an example. They provide a unique experimental set-up to study *artificial crystal* structures with tunable physical parameters. An optical lattice resembles an 'egg box'-like arrangement of single quantum wells, each confining a small number of atoms. Different lattice geometries can be realized (see [2] for a review). The tunnelling and the localization of atoms in the lattice are controlled by the lattice

PII: S1367-2630(07)36581-6
© IOP Publishing Ltd and Deutsche Physikalische Gesellschaft

depth which can be tuned by changing the laser intensity. This allows for a smooth transition from a tightly bound lattice to a system of nearly free atoms. The confined atoms have many internal (hyperfine) states which can be manipulated by laser light. In a dilute atom gas, s-wave scattering can be approximated by a contact interaction between the atoms. Its strength can be tuned in the vicinity of a Feshbach resonance [3]–[8].

For bosons in an optical lattice, it was possible to realize the Mott insulator-superfluid quantum phase transition [9], [10]–[12]. More recently, a fermionic many-particle quantum system on a three-dimensional (3D) lattice was experimentally studied by Köhl *et al* [13, 14], who investigated the interaction-driven transitions between the lowest bands. It has been proposed that a Hund's rule-like coupling between the lowest bands would lead to antiferromagnetic (AF) order [15].

The atom dynamics in an optical lattice is often described by the Hubbard or the Bose–Hubbard models [9, 16, 17]. In a deep lattice, for a half-filled band, or one fermion per site, the Hubbard model predicts antiferromagnetism. In this case, the Hubbard Hamiltonian coincides with the AF Heisenberg model of localized atoms [18]. When the band is filled, each lattice site carries two fermions with opposite spins, and magnetism can not be observed. More recently, a SU(n) Hubbard model was applied to describe fermionic atoms with n different 'flavours' or spin states [19].

Here, we show that optical lattices with a few ($N \leqslant 12$) fermionic atoms per lattice site with two hyperfine, or spin, species have an intriguing and rich magnetic structure.

The magnetism follows closely the shell structure in the individual lattice wells, emerging as there is an excess of one spin species at a single lattice site. The situation is in fact, analogous to the behaviour of quantum dot lattices in semiconductors, where the magnetism is governed by the shell structure of the single-dot components [20]–[22].

A 2D optical lattice can be created by counter-propagating laser beams. The resulting potential is a sinusoidal standing wave

$$V_{\mathrm{opt}}(\mathbf{r}) = V_0(\cos^2(kx) + \cos^2(ky)), \tag{1}$$

where the amplitude V_0 is tuned by laser intensity and the wave number $k = 2\pi/\lambda$ is set by the laser wavelength [10]. A natural unit for the energy is the recoil energy $E_{\mathrm{R}} = \hbar^2k^2/(2m)$, and length is measured by the inverse of the wavenumber. (In experiments, an underlying slowly varying harmonic confinement is added giving rise to an inhomogeneous filling of the lattice and coexistence of insulating and conducting domains. This external confinement can be made small and is neglected here.)

We consider a square lattice with two lattice sites in the unit cell, as sketched in figure 1(A) and (B). One site resides at the centre of the unit cell, and the other one crosses the corner periodically, as indicated in the contour plot of the optical potential. Note that this is the simplest choice of the unit cell allowing for AF alignment of the single-site spins. The inter-site tunnelling can be tuned by varying the lattice depth V_0. With increasing V_0 the atoms become more localized at the lattice sites, the band dispersion decreases and the shells in the individual traps are separated by increasingly large gaps. For sufficiently large lattice depth V_0, it is the shell structure of the the individual atom traps at the lattice sites that determines the physical behaviour of the lattice.

The mechanism leading to magnetic effects in the individual quantum wells of the lattice is sketched in figure 1(C). In the two-component contact-interacting fermion gas, due to the Pauli principle there is no mutual interaction between the same-species atoms. Therefore, the trapped

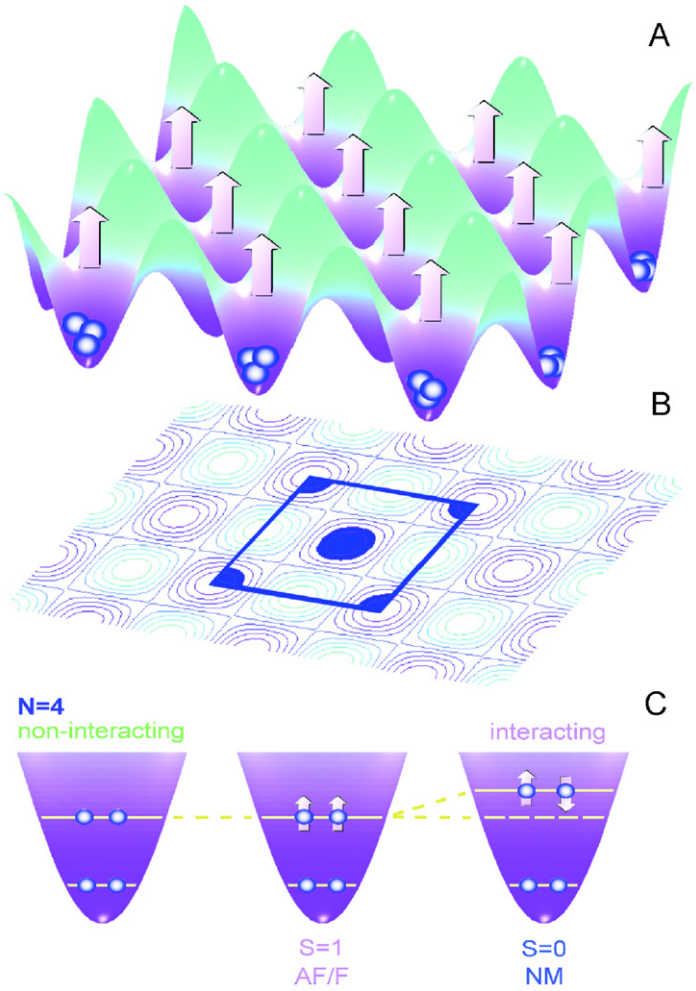

Figure 1. (A) Schematic sketch of the optical lattice potential, $V_{\rm opt}$, confining a small number of atoms in each of the potential minima. (Here, the arrows indicate a ferromagnetic (F) ground state as an example.) (B) shows the contours of $V_{\rm opt}$ and indicates the unit cell, with one trap at the centre of the unit cell, and the second one crossing the corner of the cell periodically. (C) Illustration of Hund's first rule with repulsive contact interactions: the energy is lower as the particles become non-interacting for the same species, i.e., aligned spins (see text).

atoms at a degenerate shell can lower their interaction energy by maximizing the number of atoms of the same species—in other words, by aligning their spins. This mechanism in contact-interacting fermionic systems leads to Hund's first rule [23] and magnetism, in close similarity to long-range interacting electronic systems, as for example, quantum dots in semiconductor heterostructures [24]. Here, however, Hund's rule has a more dramatic effect since it removes completely the interaction between atoms of the same species.

A Bose–Einstein condensate of a weakly interacting, dilute gas of bosonic atoms is known to be well described by the Gross–Pitaevskii equation for the condensate wavefunction [25]. Correspondingly, in the dilute limit, contact-interacting fermions may be approximated by a set of Kohn–Sham-like equations with an exact local exchange potential [26]. Periodic boundary

conditions imply Bloch form for the orbitals, $\psi_{n\mathbf{k}\sigma}(\mathbf{r}) = \exp(\mathrm{i}\mathbf{k}\cdot\mathbf{r})u_{n\mathbf{k}\sigma}(\mathbf{r})$, where n labels the band, $\sigma = (\downarrow, \uparrow)$ is the spin index and the wavevector $\mathbf{k}$ is confined into the first Brillouin zone. The periodic functions $u_{n\mathbf{k}\sigma}(\mathbf{r})$ satisfy

$$-\frac{\hbar^2}{2m}(\nabla + i\mathbf{k})^2 u_{n\mathbf{k}\sigma}(\mathbf{r}) + [V_{\mathrm{opt}}(\mathbf{r}) + gn^{\sigma'}(\mathbf{r})]u_{n\mathbf{k}\sigma}(\mathbf{r}) = \varepsilon_{n\mathbf{k}\sigma}u_{n\mathbf{k}\sigma}(\mathbf{r}), \quad \sigma \neq \sigma', \tag{2}$$

where m is the atom mass, n^σ is the density of atom species σ and g is the interaction strength. For the latter we have set $g = 0.15\, E_{\mathrm{R}}/k^2$ in order to stay in the weak-interaction regime, where equation (2) is valid. (This was confirmed by comparing the mean-field calculations for a single 2D harmonic trap with results obtained by exact diagonalization for $N \leqslant 8$, see [27].) The diluteness of the system is defined by the ratio of the interaction energy integrated over a unit cell, $E_i = \int n^\uparrow n^\downarrow \mathrm{d}^2 r$, and the Fermi energy E_{F}. This ratio does not depend strongly on the lattice depth V_0 since with increasing V_0, the Fermi energy scales accordingly. For the Bloch wavevector we use a mesh of 5×5 points in the first Brillouin zone, and the key results were tested with up to 9×9 points. In the band-structure calculation, the functions $u_{n\mathbf{k}\sigma}(\mathbf{r})$ are expanded in a basis of 11×11 plane waves. The self-consistent iterations were started with antiferromagnetic and ferromagnetic initial potentials and small random perturbations were added to the initial guesses in order to avoid convergence into saddle points of the potential surface.

The results of the calculations in the above scheme are displayed in figure 2, which shows the systematics of the magnetism as a function of the shell filling of the single quantum wells in the lattice—as a function of number of fermions per potential minimum (or lattice site) N—and the depth of the optical potential V_0. The calculated points and the different ground state configurations are indicated explicitly in the figure. Filled and open circles are the antiferromagnetic (AF) and ferromagnetic (F) states, respectively. As can be seen from the figure, for small enough values of V_0, the lattice becomes NM for all particle numbers as tunnelling between the sites dominates. The NM states are indicated by squares.

The different magnetic phases follow systematically the filling of the single-trap shell structure.

A single minimum of the trapping potential (1) can be approximated by a 2D harmonic potential with $\hbar\omega = \sqrt{4V_0 E_{\mathrm{R}}}$. This leads to the lowest closed shells at particle numbers $N = 2$, 6, and 12 (which are frequently also called 'magic numbers' in the literature, referring back to the conventions in nuclear physics) [1]. At higher energies, however, the potential (1) has a notch connecting the different lattice sites which imposes a square symmetry that breaks the three-fold degeneracy of the third, 2s1d, oscillator shell. Due to this notch, the non-interacting energies deviate from the harmonic shell structure and the closed shells correspond now to atom numbers $N = 2$, 6, 10 and 12. At magic numbers, the spins in the single quantum wells located at the minima of the optical potential are compensated, and the lattice is non-magnetic (NM). However, in between these values, at $N = 1, 4, 8$ and 11, the shells are *half-filled.* Antiferromagnetic (AF) ordering of spins is observed as a gap is formed at the Fermi level, since the nearest similar neighbour is twice as far away as in the ferromagnetic (F) lattice where every lattice site is identical. For other atom numbers, the shells are only partially filled, and therefore the Fermi levels reside in the middle of a band. These configurations cannot open a gap. They favour ferromagnetism, as the exchange-like effect splits the spin levels. The lowest band is formed from the 1s levels of the individual wells. It can be occupied by at most two atoms per lattice site. At half-filled band, ($N = 1$), the AF ordering of spins opens a Fermi gap.

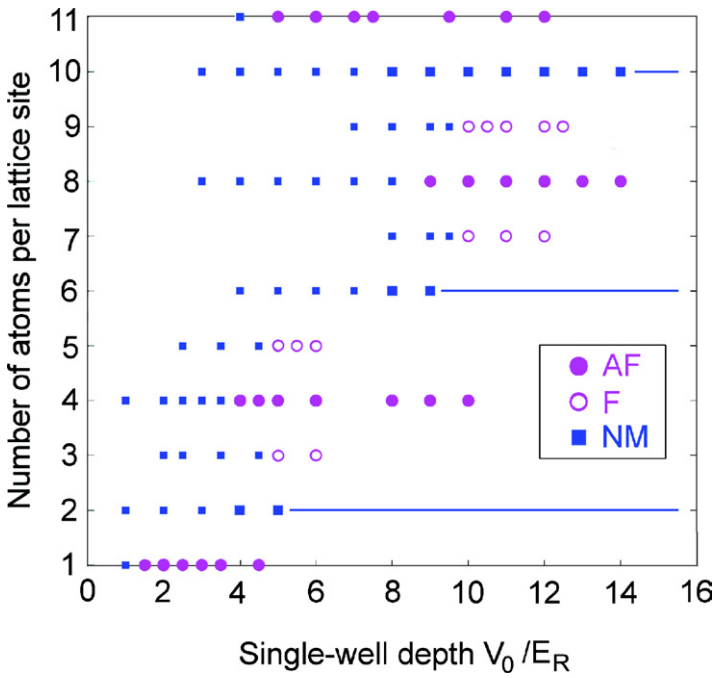

Figure 2. Magnetism in a square optical lattice, as a function of the lattice depth V_0 (determining the tunnelling and coupling between the single wells) in units of the recoil energy E_R, and the particle number per lattice site minimum N (determining the shell filling). The different non-magnetic (NM, *blue squares*), F (*empty circles*) and AF (*filled circles*) phases are indicated. For closed shells ('magic numbers') at $N = 2$, 6 and 10, the lattice is NM. The AF ground state is seen at mid-shell only, i.e., at $N = 1$, 4 and 8. In between, i.e., at the beginning and end of a shell, the lattice is F. There is a NM region at smaller values of V_0 for all particle numbers.

For $N = 3$, 4, 5 and 6 the levels at the 1p shell are occupied. At $N = 4$ the spin at the 1p shell is maximized due to Hund's first rule. This mid-shell configuration favours antiferromagnetism where the energy is reduced by opening the Fermi-gap. At $N = 3$ the shell has only one atom in a p-shell and at $N = 5$ the shell is nearly filled. In both these cases the Fermi-energy lies on the band and ferromagnetism is found.

At the third shell, 2s1d, a shell closing at $N = 10$ with a NM phase, and mid-shell fillings for $N = 8$ and $N = 11$ with AF phases are encountered. This is attributed to the symmetry-breaking due to a potential junction connecting different lattice sites. The d-state whose density lobes are not oriented towards the nearest neighbours is pushed higher in energy. As a result, the 2s1d shell is split into two sub-shells, one consisting of 2s and 1d levels and the other one formed by the higher-lying 1d level. This removal of degeneracy of the third shell in the non-interacting system can be modeled by perturbing a single 2D harmonic well with a square potential. To confirm this, we performed a first order degenerate perturbation theory calculation on the third shell. We found a similar separation into two sub-shells.

In this paper, we studied fermions with spin $1/2$ as the most simple example. As we are not aware of experimental results in this case, we compare the relevant energy scales to the fermionic

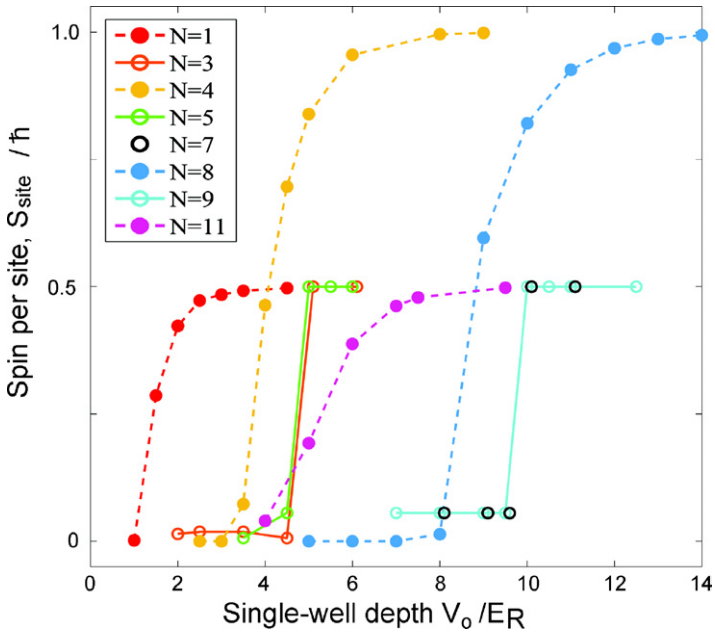

Figure 3. Integrated spin density over a single lattice site ('spin per site', $S_{\text{site}}/\hbar$), as a function of increasing lattice depth V_0 (in units of the recoil energy E_{R}). The different colours correspond to different particle numbers (shell fillings) of the single traps, as indicated in the inset.

potassium gas. The splitting between the spin bands in the F cases is of the order of $0.050E_{\text{R}}$ which corresponds to approximately $0.048k_{\text{B}}T_{\text{F}}$ in a gas of ^{40}K, where the Fermi temperature is $T_{\text{F}} = 330$nK [28]. The typical energy difference between NM and F states is $0.001E_{\text{R}}$, corresponding to roughly $0.001k_{\text{B}}T_{\text{F}}$ in the fermionic potassium gas. These energies correspond to temperatures which are about a factor of ten lower than the ones achieved experimentally. We mention here that an interaction-induced cooling mechanism was proposed in order to reach the AF phase at $N = 1$ [29].

The onset of magnetism as a function of V_0 can be seen in figure 3 which shows the 'spin per site', obtained by integrating the spin density over a single lattice site

$$S_{\text{site}} = \frac{\hbar}{2}\int_{\text{site}} [n^{\uparrow}(\mathbf{r}) - n^{\downarrow}(\mathbf{r})]\,\mathrm{d}\mathbf{r}. \tag{3}$$

Generally, the magnetism sets on with increasing V_0 as the number of atoms per lattice site becomes larger, and thus the spatial extent of the highest occupied orbital increases. The transition occurs roughly at the same value of V_0 when the Fermi level resides at particular shells. For example, the transition occurs at $V_0 \approx 4.2\ E_{\text{R}}$ for atom numbers $N = 3$, 4 and 5 as the 1p levels are occupied. For $N = 11$ atoms, antiferromagnetism sets on already around $V_0 = 5\ E_{\text{R}}$. In this case, the highest occupied orbital (1d) has only a small overlap with the corresponding orbital at the neighbouring site. Therefore, the optical lattice has to be shallow before the tunnelling between these levels is large enough for the magnetism to disappear.

In an optical lattice, one need not have an integer number of atoms per lattice site. Likewise, since we consider an extended lattice, there is no restriction to an integer number of particles

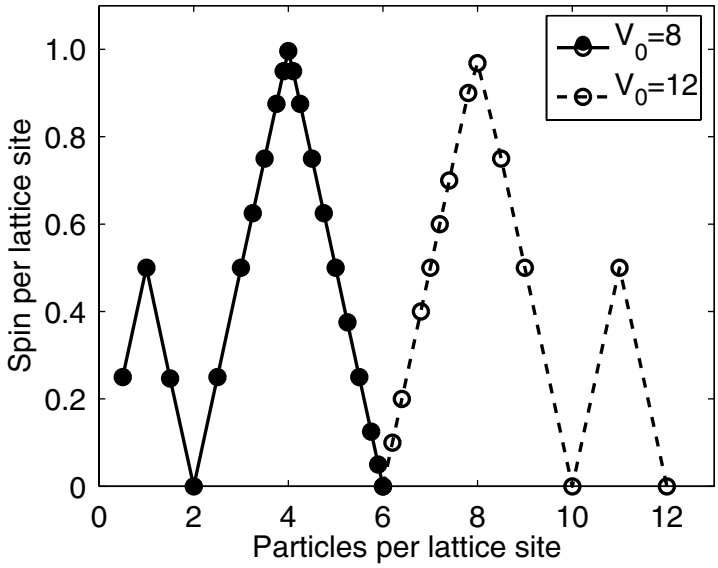

Figure 4. Spin per lattice site as a function of number of atoms per site at fixed lattice depth $V_0 = 8\ E_R$ for $N = 0.5 - 6$ (solid line) and $V_0 = 12\ E_R$ for $N = 6 - 12$ (dashed line).

per unit cell either. Consequently, any (integer or non-integer) number of atoms per lattice site is permissible. A complete and detailed phase diagram for the optical lattice should therefore include also systematic study of non-integer particle numbers.

To shed some light on the physics of the lattice at non-integer filling we have performed calculations for some sample parameter values. Figure 4 shows the spin per lattice site as a function of the number of atoms per site, for fixed lattice depth. (This quantity is obtained by integrating the spin density over a single lattice site according to equation (3).) The lattice depth ($V_0 = 8E_R$ for $0.5 \leqslant N \leqslant 6$ and $V_0 = 12E_R$ for $6 \leqslant N \leqslant 12$) is chosen such that the system is always in the tightly-bound limit, where magnetism is seen. The figure shows clearly how the spin per site, and hence magnetization, rises linearly from zero at atom numbers corresponding to closed shells to a maximum at mid-shell, and then drops back to zero again.

We note also that when the lattice is magnetic, it is always F, except precisely at the atom numbers corresponding to half-filled shells. Another interesting exception is found at $N = 1.5$: if the lattice is deep enough, a magnetized state will form, where two atoms sit at one of the sites of the unit cell, their spins cancelling, and the third atom sits at the other site. This forms a ferrimagnetic-like state. The mean spin per site is then 0.25, as depicted in figure 4. Our preliminary Hubbard-model calculations confirm this picture, but indicate that the true state may be an '*anti*-ferrimagnetic' state instead (where every second site again has zero spin, but where the sites with spin form an AF spin order within their sub-lattice, a state which cannot be described with the two-site unit cell used in this study). Similar states with ferrimagnetic-like spin order occur also for $N = 5.5, 9.5$ and 11.5, i.e., at 0.5 particles short of a filled shell. The transition to the ferrimagnetic-like state is gradual over a range of V_0 values, as V_0 increases for fixed N.

In summary, we found that two-component cold fermionic atoms in an optical lattice establish a rich magnetic phase diagram, and can show effects analogous to the electrons in

magnetic solids. The magnetism in the optical lattice is determined by the number of atoms per lattice site, and the depth of the lattice. If the lattice is shallow, for strong inter-site tunnelling the lattice does not show any magnetism. For deeper lattices, where the tunnelling is small, the total spin of the N atoms at the single sites is determined by the shell structure in the lattice minima. For closed shells (so-called 'magic numbers') at $N = 2, 6, 10$ and 12, the individual traps are NM. For contact-interacting repulsive fermions, Hund's first rule applies in a particularly dramatic way, removing the interaction between same-species atoms. AF ordering of the single-site spins is found when a gap at the Fermi level can open. This is the case at mid-shell, with $N = 1, 4, 8$, or 11 particles in the single traps. Ferromagnetism occurred at the beginning and the end of a shell. Studies of non-integer fillings in the magnetized region of the phase diagram show that magnetization depends linearly on the number of atoms per site, and that the magnetic structure is always ferromagnetic, except exactly at numbers corresponding to filled and half-filled shells of the individual traps.

Acknowledgments

This study was financially supported by the Swedish Research Council, the Swedish Foundation for Strategic Research, the Finnish Academy of Science, and the European Community project ULTRA-1D (NMP4-CT-2003-505457).

References

[1] Reimann S M and Manninen M 2002 *Rev. Mod. Phys.* **74** 1283
[2] Jaksch D and Zoller P 2005 *Ann. Phys.* **315** 52
[3] Feshbach H 1958 *Ann. Phys.* **5** 337
[4] Inouye S, Andrews M R, Stenger J, Miesner H-J, Stamper-Kurn D M and Ketterle W 1998 *Nature* **392** 151
[5] Courteille Ph *et al* 1998 *Phys. Rev. Lett.* **81** 69
[6] Roberts J L *et al* 1998 *Phys. Rev. Lett.* **81** 5109
[7] Duine R A and Stoof H T C 2004 *Phys. Rep.* **396** 115
[8] Theis M, Thalhammer G, Winkler K, Hellwig M, Ruff G, Grimm R and Hecker Denschlag J 2004 *Phys. Rev. Lett.* **93** 123001
[9] Jaksch D, Brunder C, Cirac J I, Gardiner C W and Zoller P 1998 *Phys. Rev. Lett.* **81** 3108
[10] Greiner M, Mandel O, Esslinger T, Hänsch T W H and Bloch I 2002 *Nature* **415** 39
[11] Stöferle T, Moritz H, Schori C, Köhl M and Esslinger T 2004 *Phys. Rev. Lett.* **92** 130403
[12] Xu K, Abo-Shaer J R, Mukaiyama T, Chin J K, Miller D E, Ketterle W, Jones K M and Tiesinga E 2005 *Phys. Rev.* A **72** 043604
[13] Köhl M, Moritz H, Stöferle T, Günter K and Esslinger T 2005 *Phys. Rev. Lett.* **94** 080403
[14] Köhl M, Günter K, Stöferle T, Moritz H and Esslinger T 2006 *Preprint* cond-mat/0605099
[15] Ho A F 2006 *Phys. Rev.* A **73** 061601
[16] Lewenstein M, Sanpera A, Ahufinger V, Damski B, Sen De A and Sen U 2006 *Preprint* cond-mat/0606771
[17] Drummond P D, Corney J F, Liu X-J and Hu H 2005 *J. Mod. Opt.* **52** 2261–8
[18] Vollhardt D 1994 *Perspectives in Many-Body Physics* ed R A Broglia, J R Schrieffer and P F Bortignon (Amsterdam: North-Holland)
[19] Honerkamp C and Hofstetter W 2004 *Phys. Rev. Lett.* **92** 170403
[20] Koskinen M, Reimann S M and Manninen M 2003 *Phys. Rev. Lett.* **90** 066802
[21] Koskinen P, Sapienza L and Manninen M 2003 *Phys. Scr.* **68** 74
[22] Kolehmainen J, Reimann S M, Koskinen M and Manninen M 2000 *Eur. Phys. J.* B **13** 731

[23] Weissbluth M 1978 *Atoms and Molecules* (New York: Academic)
[24] Koskinen M, Manninen M and Reimann S M 1997 *Phys. Rev. Lett.* **79** 1389
[25] Dalfovo F, Giorgini S, Pitaevskii L P and Stringari S 1999 *Rev. Mod. Phys.* **71** 463
[26] Magyar R J and Burke K 2004 *Phys. Rev.* A **70** 032508
[27] Yu Y *et al*, unpublished.
[28] Pezz L, Pitaevskii L, Smerzi A, Stringari S, Modugno G, de Mirandes E, Ferlaino F, Ott H, Roati G and Inguscio M 2004 *Phys. Rev. Lett.* **93** 120401
[29] Werner F, Parcollet O, Georges A and Hassan S R 2005 *Phys. Rev. Lett.* **95** 056401